

Date of publication xxxx 00, 0000, date of current version xxxx 00, 0000.

Digital Object Identifier 10.1109/ACCESS.2020.DOI

Throughput Analysis of Multipair Two-way Relaying Networks with NOMA and Imperfect CSI

DINH-THUAN DO¹ (Senior Member, IEEE), THANH-LUAN NGUYEN², KHALED M. RABIE³, XINGWANG LI (Senior Member, IEEE)⁴, AND BYUNG MOO LEE⁵, (Member, IEEE)

¹Wireless Communications Research Group, Faculty of Electrical & Electronics Engineering, Ton Duc Thang University, Ho Chi Minh City 700000, Vietnam

²Faculty of Electronics Technology, Industrial University of Ho Chi Minh City (IUH), Ho Chi Minh City 700000, Vietnam.

³Department of Engineering, Manchester Metropolitan University, Manchester M1 5GD, U.K.

⁴School of Physics and Electronic Information Engineering, Henan Polytechnic University, Jiaozuo 454003, China.

⁵School of Intelligent Mechatronics Engineering, Sejong University, Seoul, 05006, Korea.

Corresponding author: Dinh-Thuan Do (e-mail: dodinhthuan@tdtu.edu.vn), Byung Moo Lee (e-mail: blee@sejong.ac.kr)

This work was supported by the Basic Science Research Program through the National Research Foundation of Korea (NRF) funded by Korea government (MSIT) (Grant No.: NRF-2020R1F1A1048470) (Grant No.: NRF-2019R1A4A1023746).

ABSTRACT To improve the utilization of spectrum and system capacity, non-orthogonal multiple access (NOMA) is considered as a promising multiple access method for emerging communication technologies. Its advantageous benefits are implemented in two-way wireless networks. Power allocation factors assigned to multiple users play a key role in the successful deployment of fairness balance in NOMA. This paper considers fixed power allocation, and performance degradation is predicted in worse situation in which non-optimal power scheme and the imperfect channel state information (CSI) happen. More challenging issue happens in this system, and this paper addresses the situation of NOMA supporting multi-pair of users, in which group of users can communicate to other users to achieve acceptable throughput in two kinds of mode, i.e. delay-limited mode and delay-tolerant mode. Two performance metrics have been considered, namely, ergodic rate and outage probability. For both metrics, we derived closed-form analytical expressions as well as asymptotic performance. Numerical results show that the proposed system presents benefits to cellular networks by extending ability to serve more users who have different demands on data communication. Monte Carlo simulations are provided throughout to validate the accuracy of the derived analytical expressions.

INDEX TERMS two-way relaying networks, non-orthogonal multiple access, imperfect channel state information, outage probability, ergodic rate

I. INTRODUCTION

Recently, the introduction of emerging multimedia applications for wireless networks suffers from a significant massive users requirements and the dramatic rise data transmission [1]. Non-orthogonal multiple access (NOMA) has recently attracted a lot of research attention to meet such increasing needs and the main requirements such as low latency and massive connectivity. NOMA is proposed due to its advantages of achieving reduced access latency, enhanced user fairness, enlarged connections, and facilitated diverse quality of service (QoS) [2]. Different users in NOMA system occupy the same time, frequency and spreading code domain, different power levels. To guarantee that individual signals can be detected at receivers, different power allocation fac-

tors is exploited to serve users [3]. The most important aspect in NOMA is that signals from different users are superimposed at the transmit side and then transmitted over the same frequency resource at the same time slot. Successive interference cancellation (SIC) is necessary to detect signal at the receiver sides [4]. NOMA can also provide better system throughput in comparison to the conventional orthogonal multiple access (OMA) in term of the system throughput. Furthermore, NOMA provides improved scheme to reduce outage probability [5], [6]. Different from other kinds of multiple access techniques, NOMA users with weaker channel conditions need more allocated power and hence NOMA maintains the user fairness [7]- [9]. Furthermore, due to the ability to provide spatial diversity gain, cooperative commu-

nication has been introduced to improve system performance metrics [10], such as coverage and the communication reliability [11]. Therefore, cooperative networks and NOMA are required to form cooperative NOMA (CNOMA). CNOMA has been proposed as an efficient mean of improving the system efficiency and the spatial diversity, which has attract a great deal of research interests [12]–[15]. The authors in [15] examined performance degradation resulted from the problem of hardware impairment-aware design and such study valuated to implement cognitive radio (CR) in the context of combining CR and NOMA scheme in practice. Besides, nodes are able to communicate with each other in CNOMA systems. To provide additional transmission opportunities to the devices, relays are necessary helpers which improve the quality of the received signals to forward to distant devices [16], [17]. Two main schemes were considered in [16]. In particular, they introduced the first scenario in which the first device intends to communicate with the second device through the assistance of Amplify-and-Forward/ Decode-and-Forward (AF/DF)-assisted base station (BS) without energy harvesting. The second scenario in [16] presented the scenario as the wireless powered device was able to communicate with a non-energy harvesting device.

Regarding relaying scheme, the two-way relay (TWR) technique is introduced as a further advance. Due to its capability to boost the spectral efficiency, TWR has attracted a remarkable interests [18]. By exchanging information between two nodes with the help of a relay, TWR networks can provide improvement in term of spectrum efficiency [19]. On the other hand, full-duplex mode is applied in CNOMA and such a network benefits from combining the application of TWR into a relevant approach to enhance the spectral efficiency of systems. The authors in [20] proposed a two-way cooperative relay scheme employing NOMA in which two users operating in three phases benefits from bidirectional communication scheme. They showed that its performance is better than a conventional one way CNOMA system in terms of outage probability and ergodic rate. With characterizations of compressing data and high spectral efficiency in Network Coding (NC), the authors in [21] introduced a hybrid concept to employ a two-way relaying system (namely Hybrid-TWRS) which combines NOMA and NC.

Considering cognitive radio NOMA (CR-NOMA) networks, they introduced a two-way full-duplex (TW-FD) relaying to achieve better energy efficiency since the self-interference (SI) of FD can be regarded as a potential source related to harvest energy. Their main results indicated maximal security energy efficiency can be obtained for the secondary user (SU) system [21]. Other investigations as in [22] and [23] showed the advantages of FD TWR-CNOMA systems. In particular, the authors of [22] examined a successive group decoding scheme and a rate splitting factor in these FD TWR-CNOMA networks, in which theoretical performance evaluation was not performed. While secure transmission including base station (BS), a trusted relay, single and multiple eavesdroppers is explored in [23] to eval-

uate secure performance of a FD TWR-CNOMA network. However, their results are limited since only the achievable ergodic rate was considered.

However, most of the aforementioned studies assumed that perfect knowledge of the channel state information (CSI) known at the receivers. However, in practice, it is hard to achieve perfect CSI because of significant system overhead related to high accuracy of channel estimation [24]. Recently, the authors in [25] considered the channel estimation error as interference to examine the outage performance of a downlink NOMA system under impacts of imperfect CSI. NOMA-based downlink AF relay network in circumstance of imperfect CSI was studied in [26]. The authors of this work assumed the situation of the high signal to noise ratio (SNR) to find floor performance of the outage probabilities since the interference of the channel estimation error made degraded performance. However, in [25] and [26], they did not show optimal performance of uplink scenario in NOMA systems as the fixed-ordered decoding scheme is implemented based on the received signal strength in the long term. Returning to decoding order, the user with higher instantaneous received power should be detected first, and then the split from the received superposed signals to detect the remaining users. The most important point is that the order of instantaneous received powers of the superposed signals vary among different time blocks [27], and the decoding order should be varied following this change. As a result, critical problems in uplink NOMA system happens as considering the influence of the incorrect channel estimation.

Moreover, there still exist several existing implementation issues in practical scenarios of NOMA with the disadvantage of imperfect CSI [28]–[31]. It is noted that these unfavorable factors are the reasons of errors in the decoding process. In [20], [22], hard problem of multiple users in two-way NOMA are still not addressed, and open problem need be addressed in terms of ability of multiple pairs of users served by principle of NOMA and practical scenario of imperfect CSI. Motivated by these, to concentrate on the two-way NOMA and imperfect CSI, it is indicated that the degraded outage performance happens due to existence of channel estimation error in this considered NOMA system. In light of the above, the main contributions of this paper are summarized as follows:

- 1) We derive closed-form expressions of the ergodic capacity for the proposed multi-pairs system based on the instantaneous signal strength with imperfect CSI condition. Reporting from the simulation, this mechanism indicates that more pairs of users results in worse performance. However, the optimal throughput can be achieved by varying target rates.
- 2) We consider more insights related to the throughput performance in two modes, namely delay-limited transmission mode and delay-tolerant transmission mode. In addition, the impact of imperfect CSI on system performance is evaluated in the context of two-way transmission for NOMA system by analyzing diversity

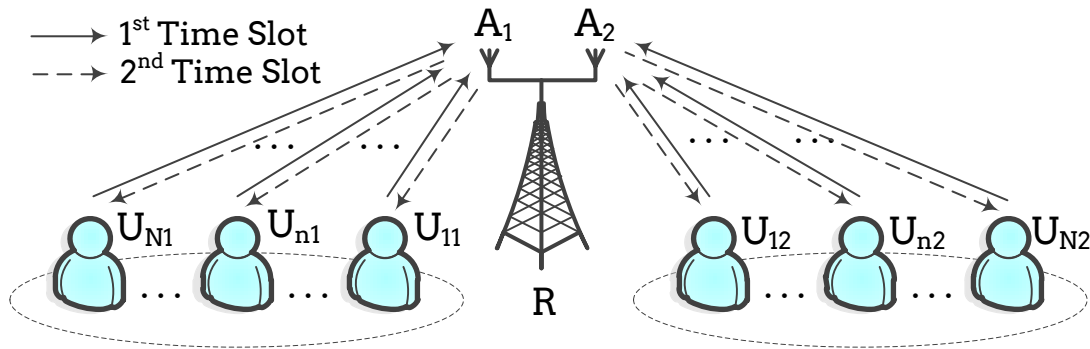


FIGURE 1. An illustration of TWR-NOMA systems, in which two groups of users exchange messages via the central relay R .

order.

- 3) Results show that under CSI imperfections, the considered TWR-NOMA scheme not only improves the spectral efficiency, but also increases throughput at several points related to power allocation factors and target rates. Moreover, it is shown that the throughput performance in delay-limited mode achieved with imperfect CSI is proven to be the best at case of 4 pairs of users. Furthermore, reducing levels of channel estimation errors achieves reasonable values of the throughput.

The remainder of this paper is organized as follows. The system model of the proposed network is presented in Section II. We formulate in Section III the throughput in two cases including delay-limited transmission mode and delay-tolerant mode as well. Numerical examples and Monte Carlo results are presented in Section IV. Finally, we draw our conclusions in Section V.

II. SYSTEM MODEL AND COMPUTATION OF RECEIVED SIGNAL

A. SYSTEM MODEL

In Fig. 1 our attentions put on the situation of two-way mode activated in NOMA network. In this system, the two-antenna relay R is main intermediate node is designed to serve N pairs of NOMA users. It is worth noting that these users are considered based on their distances to the relay node with regard to decoding order. Two groups $G_1 (U_{11}, U_{11}, \dots, U_{N1})$ and $G_2 (U_{12}, U_{22}, \dots, U_{N2})$ are facilitated under the support of a relay employing decode-and-forward (DF). It is noted that relay provides more advantages since two antennas are able to transmit and receive in the same time, namely A_1 and A_2 . To reduce hardware design at users, single antenna is equipped at users by utilizing superposition coding scheme. In practice, it has too high complexity to implement relaying mode related to decoding signal, i.e. DF protocol. However, DF protocol is assumed to ideal case to further examine more serious problem regarding CSI imperfection and ability of processing multiple pairs of users. In this model, two time slots are required to process signal at uplink and downlink in TWR-NOMA.

Additionally, to simple analysis, some assumptions need to be required. It is assumed that the direct links between two pairs of users do not exist due to the effects of serve shadowing [22]. Without loss of generality, all the wireless channels are modeled to be independent quasi-static block Rayleigh fading channels and disturbed by additive white Gaussian noise with mean power N_0 . Furthermore, we assumed that the feedback to the transmitter is instantaneous and error free, which means that CSI is also achievable at the transmitter whatever CSI the receiver has. Let the estimate for the channel h_{nk} be \hat{h}_{nk} . By assuming MMSE estimation error, it holds that [25], [26], [28]

$$h_{nk} = \hat{h}_{nk} + \tilde{h}_{nk}, \quad (1)$$

where \tilde{h}_{nk} stands for the channel estimation error and it has distribution of a complex Gaussian with zero mean and variance of δ_{nk} , i.e., $\tilde{h}_{nk} \sim \mathcal{CN}(0, \delta_{nk})$. Hence, the channel estimate \hat{h}_{nk} is also zero-mean complex Gaussian with variance $\hat{\Omega}_{nk} = d_{nk}^{-\eta} - \delta_{nk}$, in which δ_{nk} is denoted as the quality of channel estimation. In addition, the normalized channel estimation error factor is denoted as $\zeta_{nk} = \delta_{nk} d_{nk}^{\eta}$ and then the variance can be known as $\hat{\Omega}_{nk} = d_{nk}^{-\eta} (1 - \zeta_{nk})$ with $\zeta_{nk} \in [0, 1]$. It is assumed that $\hat{\Omega}_{1k} > \hat{\Omega}_{2k} > \dots > \hat{\Omega}_{Nk}$, then it helps to further determine the order of the estimated channel gains as $|\hat{h}_{1k}|^2 > |\hat{h}_{2k}|^2 > \dots > |\hat{h}_{Nk}|^2$.

B. INFORMATION PROCESSING

In this paper, a dual time slot transmission provides two-way manner for TWR-NOMA network. In particular, the NOMA users in group G_1, G_2 communicate in the first slot with R (uplink phase). Since two antennas in R provide higher bandwidth efficiency, but while the relay R receives the signals from the users in G_1 , interference signals from the pair of users in G_2 harm R .

Now, at the antenna A_k , the received signal at relay R can be expressed as

$$y_k = \sqrt{P} \sum_{n=1}^N \sqrt{\beta_{nk}} (\hat{h}_{nk} + \tilde{h}_{nk}) x_{nk} + I_k + n_k, \quad (2)$$

where P as the transmit power at the user nodes, β_{nk} specifies the uplink power control with $\beta_{1k} > \beta_{2k} > \dots > \beta_{Nk}$, x_{nk} denotes the unit energy signal transmitted by the user U_{nk} and n_k denotes the noise at the k -th antenna at R with N_0 being its variance. It is noted that $(k, \bar{k}) = (1, 2)$ or $(k, \bar{k}) = (2, 1)$. Moreover, I_k is the aggregated inter-group interference signal (IS) from $A_{\bar{k}}$ which can be given as

$$I_k = \sqrt{P} \sum_{n=1}^N \sqrt{\beta_{n\bar{k}}} f_{n\bar{k}}^{(1)} x_{n\bar{k}}, \quad (3)$$

where $f_{n\bar{k}}^{(1)} \sim \mathcal{CN}(0, \xi_1 \Omega_{n\bar{k}})$ with $\xi_k \in [0, 1]$ specifying the impact levels of IS at R .

By means of SIC, R successively decodes U_{nk} 's information x_{nk} ($N \geq n \geq 1$) while treating other x_{mk} 's ($N \geq m \geq n+1$), as interference. Hence, the received signal-to-interference-plus-noise ratio (SINR) at R to detect x_{nk} then it is given by

$$\gamma_{R \rightarrow x_{nk}} = \frac{\beta_{nk} \phi_{nk}}{\sum_{m=n+1}^N \beta_{mk} \phi_{mk} + \iota_k + \Delta_k + 1}, \quad (4)$$

where $\phi_{nk} \triangleq \bar{\gamma} |\hat{h}_{nk}|^2$ in which $\bar{\gamma} \triangleq \frac{P}{N_0}$ is the average transmit SNR, $\iota_k \triangleq \sum_{n=1}^N \bar{\gamma} \beta_{n\bar{k}} |f_{n\bar{k}}^{(1)}|^2$ and $\Delta_k \triangleq \sum_{n=1}^N P \delta_{nk}$ is the aggregated interference due to imperfect channel estimation. Each time x_{nk} is correctly decoded, i.e., $\gamma_{R \rightarrow x_{nk}} \geq \tau_{nk}$ where $\tau_{nk} \triangleq 2^{2R_{nk}} - 1$ with R_{nk} being the data rate of x_{nk} in bit-per-channel use (BCPU), the relay then utilizes SIC to alleviate interference term then decodes the information signal of the $(n+1)$ -th user successively until x_{Nk} is decoded. The received SINR at R to detect x_{Nk} is given by

$$\gamma_{R \rightarrow x_{Nk}} = \frac{\beta_{Nk} \phi_{Nk}}{\iota_k + \Delta_k + 1}. \quad (5)$$

In the second time slot, the information is exchanged between G_1 and G_2 by the assistance of the relay R . Therefore, just as downlink NOMA, R transmits the superposed signals $\sqrt{P} \sum_{n=1}^N \sqrt{\alpha_{n1}} x_{n1}$ and $\sqrt{P} \sum_{n=1}^N \sqrt{\alpha_{n2}} x_{n2}$ to G_2 and G_1 by A_2 and A_1 , respectively, where α_{nk} denotes the power allocation of U_{nk} . In particular, to ensure the fairness between users in G_k , a higher power is allocated to the distant user who has the worse channel condition. Hence, we assume that $\alpha_{Nk} \geq \dots \geq \alpha_{2k} \geq \alpha_{1k}$. This paper limits research object by employing the fixed power allocation for two groups' NOMA users.¹

By exploiting channel reciprocal, the received signal at the nk -th user in the group G_k is given by

$$y_{nk} = \sqrt{P} \sum_{n=1}^N (\hat{h}_{nk} + \tilde{h}_{nk}) \sqrt{\alpha_{nk}} x_{nk} + I_{nk} + n_k, \quad (6)$$

¹Optimal power allocation factor will introduced to further improve the performance of systems, however, it is beyond the scope of this paper.

in which I_{nk} specifies the aggregated IS at the k -th antenna² which can be given by

$$I_{nk} = \sqrt{P} f_{n\bar{k}}^{(2)} \sum_{m=1}^N \sqrt{\alpha_{m\bar{k}}} x_{m\bar{k}}, \quad (7)$$

where $f_{n\bar{k}}^{(2)}$ is modeled by $\mathcal{CN}(0, \xi_2 \Omega_{n\bar{k}})$.

As normal principle of NOMA protocol, SIC is employed and the received SINR at U_{nk} to detect $x_{m\bar{k}}$ is given by

$$\gamma_{nk \rightarrow m\bar{k}} = \frac{\alpha_{m\bar{k}} \phi_{nk}}{\hat{\alpha}_{m\bar{k}} \phi_{nk} + \iota_{nk} + \Delta_{nk} + 1}, \quad (8)$$

where $\Delta_{nk} \triangleq \bar{\gamma} \delta_{nk}$, $\hat{\alpha}_{m\bar{k}} \triangleq \sum_{t=1}^{m-1} \alpha_{t\bar{k}}$ and $\iota_{nk} \triangleq \bar{\gamma} |f_{n\bar{k}}^{(2)}|^2$. From the above process, the exchange of information is achieved between the NOMA users who belong to groups, namely G_1 and G_2 . More specifically, the signal x_{nk} of U_{nk} is exchanged with the signal $x_{n\bar{k}}$ of $U_{n\bar{k}}$.

III. SYSTEM PERFORMANCE ANALYSIS

A. OUTAGE PROBABILITY OF x_{nk}

To look at the system performance, the performance of TWR-NOMA is further characterized in terms of outage probabilities. Due to the channel's reciprocity, it is important to consider firstly on the outage probability of x_{nk} as below.

In such a TWR-NOMA system, the outage event of x_{nk} can be explained via its complementary events those are i) the event x_{nk} is decoded correctly by the relay R and ii) the events all users U_{mk} ($n \geq m \geq 1$) correctly decode x_{nk} . The imperfect CSI situation certainly makes crucial affect on system performance. Particularly, the outage probability of x_{nk} with imperfect CSI for TWR-NOMA system can be given by

$$P_{nk}^{ip,out} = 1 - P_1 P_2, \quad (9)$$

in which P_1 and P_2 denote the probabilities for the first and the second complementary events, respectively, which are formulated by

$$P_1 = \Pr \left\{ \bigcap_{m=1}^n \gamma_{R \rightarrow x_{mk}} \geq \tau_{mk} \right\}, \quad (10)$$

$$P_2 = \prod_{m=1}^n \Pr \left\{ \bigcap_{t=n}^N \gamma_{mk \rightarrow t\bar{k}} \geq \tau_{t\bar{k}} \right\}. \quad (11)$$

To solve $P_{nk}^{ip,out}$, it needs more helps from simple computations. Therefore, the following lemma provides the outage probability of x_{nk} for TWR-NOMA in an analytical manner.

Lemma 1: *The closed-form expression for the outage probability of x_{nk} of TWR-NOMA with imperfect CSI is given by (12) in the top of the next page, in which $\lambda_{nk} \triangleq \bar{\gamma} \Omega_{nk}$,*

²Unlike [32], where inter-group interference in the first and second time slots are dependent, the interference I_k and I_{nk} are independent. This assumption is certainly not only tractable analysis it is not object from the results in [32] with low IS levels, i.e., $\xi_1, \xi_2 \approx 0$.

$$P_{nk}^{ip,out} = 1 - \prod_{m=1}^n \frac{1}{\beta_{mk} \hat{\lambda}_{mk} \Lambda_{mk}} \left\{ \sum_{m=1}^N \chi_{m\bar{k}} \left(1 + \xi_1 \beta_{m\bar{k}} \lambda_{m\bar{k}} \sum_{t=1}^n \tau_{tk} \Lambda_{tk} \right)^{-1} \right\} \exp \left(- (\Delta_k + 1) \sum_{m=1}^n \tau_{mk} \Lambda_{mk} \right) \times \left\{ \prod_{m=1}^n \left(1 + \frac{\xi_2 \lambda_{mk}}{\hat{\lambda}_{mk}} \theta_{n\bar{k}} \right)^{-1} \exp \left(- \theta_{n\bar{k}} \frac{\Delta_{mk} + 1}{\hat{\lambda}_{mk}} \right) \right\} \prod_{t=n+1}^N \left(1 + \beta_{tk} \hat{\lambda}_{tk} \sum_{m=1}^n \tau_{mk} \Lambda_{mk} \right)^{-1}, \frac{\alpha_{t\bar{k}}}{\hat{\alpha}_{m\bar{k}}} > \tau_{t\bar{k}}, \forall t, \quad (12)$$

$\hat{\lambda}_{nk} \triangleq \bar{\gamma} \hat{\Omega}_{nk}$, $\theta_{nk} \triangleq \max[(\varepsilon_{t\bar{k}})_{t=n}^N]$ where $\varepsilon_{t\bar{k}} \triangleq \frac{\tau_{t\bar{k}}}{\alpha_{t\bar{k}} - \tau_{t\bar{k}} \hat{\alpha}_{t\bar{k}}}$

$$\chi_{n\bar{k}} = \prod_{m=1, m \neq n}^N \left(1 - \frac{\beta_{mk} \lambda_{m\bar{k}}}{\beta_{nk} \lambda_{n\bar{k}}} \right)^{-1}, \quad (13)$$

and the term Λ_{mk} can be expressed in a recursive form as

$$\Lambda_{mk} = \begin{cases} \frac{1}{\beta_{1k} \hat{\lambda}_{1k}}, & m = 1 \\ \frac{1}{\beta_{mk} \hat{\lambda}_{mk}} + \sum_{t=1}^{m-1} \tau_{tk} \Lambda_{tk}, & m \geq 2 \end{cases} \quad (14)$$

Proof: See Appendix A.

Remark 1: From this interesting result, outage probability for the proposed TWR-NOMA is investigated. Considering that the channel gains information is prior known, outage probability depends on fixed power allocation factors. It is predicted that outage behavior may vary significantly due to impacts of power factors and CSI imperfection levels. Based on (12), the outage probability of x_{nk} for TWR-NOMA with perfect CSI can be obtained by substituting $\delta_{nk} = 0, \forall n, \forall k$.

B. ASYMPTOTIC ANALYSIS

In order to gain deeper insights in considered system, the asymptotic analysis are presented in the high SNR regimes based on the derived outage probabilities. The diversity order is defined as [33]

$$DO_{nk} = \lim_{\bar{\gamma} \rightarrow \infty} \frac{\log(P_{nk}^{ip,out}(\bar{\gamma}))}{\log(\bar{\gamma})}. \quad (15)$$

Based on the analytical result in (12), the asymptotic outage probability of x_{nk} for imperfect CSI can be obtained by noticing that $\Delta_k + 1 \rightarrow \Delta_k$ in high SNR regime, i.e., when $\bar{\gamma} \rightarrow \infty$. As a result, the diversity orders of x_{nk} with imperfect CSI are equal to zero.

C. DELAY-LIMITED THROUGHPUT

In delay-limited transmission scenario, throughput can be computed based on outage probability, and in this regard, the BS transmits message to users at a fixed rate, where system throughput will be subject to wireless fading channels. Under impacts of imperfect CSI, the corresponding throughput of TWR-NOMA is formulated as

$$R_{dl} = \sum_{n=1}^N (1 - P_{n1}^{ip,out}) \bar{R}_{n1} + \sum_{n=1}^N (1 - P_{n2}^{ip,out}) \bar{R}_{n2}, \quad (16)$$

where $\bar{R}_{n1}, \bar{R}_{n2}$ are the required transmission rates.

D. ERGODIC RATE OF x_{nk}

To provide other metric regarding performance evaluation, the ergodic rate of TWR-NOMA is computed for considering the influence of signal's channel fading to target rate.

Since x_{nk} can be detected at the relay as well as at $U_{m\bar{k}}$ where $m = n, n+1, \dots, N$, successfully. By the virtue of (4) and (8), the achievable rate of x_{nk} for TWR-NOMA is written as

$$R_{nk}^{erg} = \frac{1}{2} \log_2(1 + X_{nk}), \quad (17)$$

where we have defined $X_{nk} \triangleq \min(\gamma_{R \rightarrow x_{nk}}, \gamma_{1\bar{k} \rightarrow 1k}, \gamma_{2\bar{k} \rightarrow 2k}, \dots, \gamma_{n\bar{k} \rightarrow nk})$ for brevity. Then, it can be calculated the ergodic rate of x_{nk} , the corresponding CDF of X_{nk} is presented in the following Lemma.

Lemma 2: The CDF of the random variable X_{nk} , denoted by $F_{X_{nk}}$, is presented by (18) at the top of the next page, in which $\varepsilon_{nk}(\gamma) \triangleq \frac{\gamma}{\alpha_{nk} - \gamma \hat{\alpha}_{nk}}$.

Proof: See Appendix B.

Then, the corresponding ergodic rate of x_{nk} is given by

$$R_{nk}^{erg} = \frac{1}{2 \ln 2} \int_0^{\frac{\alpha_{nk}}{\hat{\alpha}_{nk}}} \frac{1 - F_{X_{nk}}(\gamma)}{1 + \gamma} d\gamma. \quad (19)$$

It can be seen that obtaining the closed-form expression of (19) for all values of $n \in [1, N]$ is intractable, not to mention impossible. However, with $n = 1$, we can obtain the exact expression of the above equation in the following proposition.

Proposition 3: The exact closed-form is examined for the ergodic rate of $x_{1k}, \forall k$, is given as

$$R_{1k}^{erg} = \frac{1}{2 \ln 2} \sum_{t=1}^N \chi_{t\bar{k}} \sum_{m=2}^N \psi_{mk} \times \left\{ \frac{\vartheta_1}{\varpi_1} \exp\left(\frac{\mu_{1k}}{\varpi_1}\right) \text{Ei}\left(-\frac{\mu_{1k}}{\varpi_1}\right) + \frac{\vartheta_2}{\varpi_2} \exp\left(\frac{\mu_{1k}}{\varpi_2}\right) \text{Ei}\left(-\frac{\mu_{1k}}{\varpi_2}\right) + \frac{\vartheta_3}{\varpi_3} \exp\left(\frac{\mu_{1k}}{\varpi_3}\right) \text{Ei}\left(-\frac{\mu_{1k}}{\varpi_3}\right) + \frac{\vartheta_4}{\varpi_4} \exp\left(\frac{\mu_{1k}}{\varpi_4}\right) \text{Ei}\left(-\frac{\mu_{1k}}{\varpi_4}\right) \right\}, \quad (20)$$

$$F_{X_{nk}}(\gamma) = 1 - \sum_{t=1}^N \chi_{t\bar{k}} \left(1 + \frac{\beta_{t\bar{k}} \lambda_{t\bar{k}}}{\beta_{nk} \hat{\lambda}_{nk}} \xi_1 \gamma \right)^{-1} \prod_{m=n+1}^N \left(1 + \frac{\beta_{mk} \hat{\lambda}_{mk}}{\beta_{nk} \hat{\lambda}_{nk}} \gamma \right)^{-1} \exp \left(- (\Delta_k + 1) \frac{\gamma}{\beta_{nk} \hat{\lambda}_{nk}} \right) \\ \times \exp \left(- \varepsilon_{nk}(\gamma) \sum_{m=1}^n \frac{\Delta_{mk} + 1}{\hat{\lambda}_{m\bar{k}}} \right) \prod_{m=1}^n \left(1 + \frac{\xi_2}{1 - \zeta_{mk}} \varepsilon_{nk}(\gamma) \right)^{-1}, \quad \gamma < \frac{\alpha_{nk}}{\hat{\alpha}_{nk}}, \quad (18)$$

in which $\varpi_1 = 1$, $\varpi_2 \triangleq \frac{\beta_{mk} \hat{\lambda}_{mk}}{\beta_{1k} \hat{\lambda}_{1k}}$, $\varpi_3 \triangleq \xi_1 \frac{\beta_{t\bar{k}} \lambda_{t\bar{k}}}{\beta_{1k} \hat{\lambda}_{1k}}$, $\varpi_4 \triangleq \xi_2 \frac{\lambda_{1\bar{k}}}{\alpha_{1k} \hat{\lambda}_{1k}}$, $\mu_{1k} \triangleq \frac{\Delta_{1k} + 1}{\alpha_{1k} \hat{\lambda}_{1k}} + \frac{\beta_{1k} + 1}{\beta_{1k} \hat{\lambda}_{1k}}$,

$$\psi_{mk} = \prod_{i=2, i \neq m}^N \left(1 - \frac{\beta_{ik} \hat{\lambda}_{ik}}{\beta_{mk} \hat{\lambda}_{mk}} \right)^{-1}, \quad \text{and} \\ \vartheta_m = - \prod_{t=1, t \neq m}^4 \left(1 - \frac{\varpi_t}{\varpi_m} \right)^{-1}.$$

Proof: See Appendix C.

To further obtain more insightful results, we consider the special cases of x_{nk} with imperfect CSI for TWR-NOMA where there is no IS between the pair of antennas at the relay in the following part.

E. SLOPE ANALYSIS

By use of asymptotic results, we evaluate the high SNR slope in this subsection. The high SNR slope can capture the impact of various channel settings on the ergodic rate, which can be given by

$$S_{nk} = \lim_{\bar{\gamma} \rightarrow \infty} \frac{R_{nk}^{\infty, erg}(\bar{\gamma})}{\log_2(\bar{\gamma})}, \quad (21)$$

in which $R_{nk}^{\infty, erg}(\bar{\gamma})$ is the ergodic rate of x_{nk} in high SNR regime, which can be obtained via yielding $\Delta_{nk} + 1 \rightarrow \Delta_{nk}$ and $\Delta_n + 1 \rightarrow \Delta_n$ from $F_{X_{nk}}(\gamma)$. After that, substituting the achievable result into (19) to obtain the asymptotic Ergodic rate of x_{nk} . Finally, our work showed that $S_{nk} = 0, \forall k, \forall n$.

Remark 2: Due to zero slope, the ergodic rate of x_{nk} reaches throughput ceilings in the high SNR regime even if perfect CSI is obtained at both antennas. Another notable reason is that the fixed decoding order in the first phase, i.e., uplink NOMA, and the influence of IS across user groups also contribute to the exist of the throughput limits.

F. DELAY-TOLERANT THROUGHPUT

In the delay-tolerant transmission scenario, the system throughput is determined by evaluating the ergodic rate. Based on the above derived results, the corresponding throughput of TWR-NOMA is given by

$$R_{dt} = \sum_{n=1}^N (R_{n1}^{erg} + R_{n2}^{erg}). \quad (22)$$

IV. NUMERICAL RESULTS

In this section, we evaluate the performance of our proposed TWR-NOMA by presenting some numerical examples of the derived expressions above. Monte Carlo simulations are

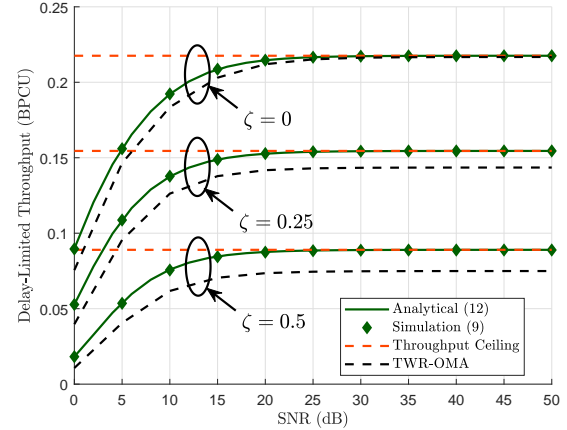


FIGURE 2. Throughput performance in delay-limited transmission mode versus SNR, in which $N = 2$, $\bar{R}_{11} = \bar{R}_{21} = 0.1$ (BPCU) and $\bar{R}_{12} = \bar{R}_{22} = 0.01$ (BPCU).

presented throughout this section to validate the correctness of these expressions. In all our evaluations, we assume that all user nodes transmit with an identical power P while all relay nodes have the same power constraint. Without any further modification, the default settings are the SI levels as $\xi_1 = \xi_2 = \xi = 0.01$, the path-loss exponent as $\eta = 2$, the distance from user U_{nk} to the relay as $1 + 9 \frac{n-1}{N-1}$ measured in meters. Regarding estimation errors, the normalized values are $\zeta_{1k} = \zeta_{2k} = \dots = \zeta_{Nk} \triangleq \zeta$, thus the nearer the user located to the relay, the less severe that user is affected by imperfect CSI. For producing NOMA, the power allocation factors are $\beta_{nk} = \frac{2^{N-n+1} - 1}{\sum_{n=1}^N (2^n - 1)}$ and $\alpha_{nk} = \frac{2^n - 1}{\sum_{n=1}^N (2^n - 1)}$.

For comparison purposes, TWR-OMA is considered in this section as a famous benchmark strategy. Particularly, the transmission takes a duration of $2N + 1$ time slots. In the first time slot, each user transmits the information signal $x_{nk}, \forall n, \forall k$, to the relay R . In the next n time slot, in which $n = 2, \dots, N, N + 1$, the relay successively transmits the signal x_{n1} to the corresponding user U_{n2} . Finally, the relay, one-by-one, transmits the symbol x_{n2} to the user U_{n1} in the remaining time slots, i.e., the $(N + 2) \div (2N + 1)$ -th time slot. The information transmission and the decoding at the relay in the first time slot of the conventional TWR-OMA network are similar to those of the proposed TWR-NOMA. Meanwhile, the relay transmits at full power in the remaining time slots for TWR-OMA. Note that the results of the dual-pair setting in this paper can be utilized to characterize the TWR-NOMA system in [32].

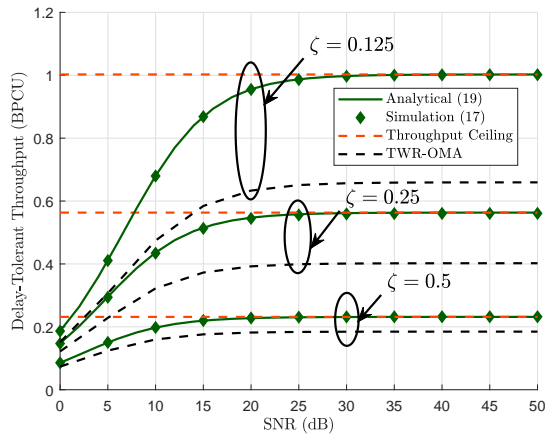


FIGURE 3. Throughput performance in delay-tolerant transmission mode versus SNR, in which $N = 2$, $\bar{R}_{11} = \bar{R}_{21} = 0.1$ (BPCU) and $\bar{R}_{12} = \bar{R}_{22} = 0.01$ (BPCU).

Fig. 2 depicts the system throughput in delay-limited transmission mode versus SNR with different normalized channel estimation errors $\zeta = 0.5, 0.25, 0$. It can be seen that the performance gaps among these cases are very small in low SNR ranges, i.e., smaller than 10 (dB). At high SNRs, ceiling throughput can be observed as SNR is greater than 30 (dB). The main reason is that the outage probability can be improved significantly at higher SNR, then corresponding throughput is enhanced accordingly. One can observe that TWR-NOMA exhibits explicit performance gaps as compared to these cases of ζ at high region of SNR. Such situation indicates that small impact of CSI can provide acceptable throughput value. The perfect CSI scenario ($\zeta = 0$) is similar to Fig. 5 reported in [32] as the performance of the dual-pair TWR-OMA and the dual-pair TWR-NOMA are similar in the high SNR regime with $N = 2$. However, in general, the proposed TWR-NOMA outperforms the conventional TWR-OMA scheme under the imperfect CSI settings.

It is shown in Fig. 3 that increasing SNR from 0 (dB) to 50 (dB), the ergodic capacity indicates upward trend. Especially, throughput increases very fast in range of SNR from 10 (dB) to 30 (dB). Moreover, in the high SNR region, the results show that TWR-NOMA converges to the throughput ceiling. Furthermore, it is worth noting that throughput in the delay-tolerant mode is higher than that of the delay-limited mode. For example, at SNR of 35 (dB), throughput under imperfect CSI in the delay-tolerant mode is 1.0 (BPCU) and such value is higher than the counterpart under perfect CSI settings. The main reason is that throughput in delay-limited mode is constrained by the threshold data rate. In addition, TWR-NOMA provides significant performance gain comparing to the considered TWR-OMA network.

The impact of the number of user pairs on throughput performance can be seen in Fig. 4. In the delay-limited mode, the throughput is somewhat improved when the number of user pairs is increased from $N = 2$ to $N = 3$, but then

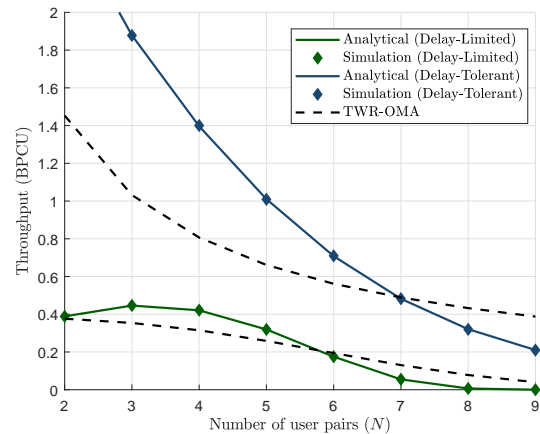


FIGURE 4. Throughput performance in two modes versus the number of user pairs, in which $\zeta = 0.01$, $\bar{R}_{n,k} = 0.2$ (BPCU), $\forall n, \forall k$, and $\bar{\gamma} = 20$ (dB).

takes a dramatic turn beyond $N = 3$. This behavior is due to the event that the relay often insufficiently allocates power for some users, which drastically reduces the performance at those users, and thus leads to a serious performance loss, especially with high values of N . Under the simulation settings, when $N = 2$, some users are over-allocated by the relay, and thus an additional pair can be deployed to make good uses of the wasted power and improve the sum-throughput. In addition, it is depicted that TWR-NOMA excellently outperforms TWR-OMA when the number of paired users is insignificant, but then underperforms TWR-OMA when N is considerably high. The reduction in the sum-throughput of TWR-OMA system is due to the additional time slots utilized for exchanging information between each group. In contrast, users in TWR-OMA systems are served with full power, regardless of the value of N , and thus perform more reliably than those in the TWR-NOMA system when there are too many users, i.e., $N \geq 6$ for the delay-limited mode and $N \geq 7$ for the delay-tolerant mode. In addition, the performance gap between the two throughput modes is driven to smaller gap by increasing the number of user pairs.

In Fig. 5, the maximum of throughput can be found as varying the threshold data rate sum rates. An exhaustive search algorithm is adopted to find the optimal power allocation ($\beta_{1k}, \beta_{2k}, \alpha_{1k}$ and α_{2k}) for each value of the rate threshold \bar{R}_{nk} (BPCU), thus then obtains the optimal sum-throughput. The outage performance is limited by higher data rate, and hence throughput is nearly zero at $\bar{R}_{nk} = 1.5$ (BPCU) for $\zeta = 0.1$, at $\bar{R}_{nk} = 2.25$ (BPCU) for $\zeta = 0.01$ and at $\bar{R}_{nk} > 2.5$ (BPCU) for the perfect CSI scenario. It is seen from the figure that throughput converges to a very low value at some points of data rates and such situation results in different quality requirements. Interestingly, Fig. 6 shows that the maximum throughput in delay-limited mode can be found in numerical method, it happens as $\alpha_{1k} = 0.3$ while it is not existence of optimal for throughput in delay-tolerant mode.

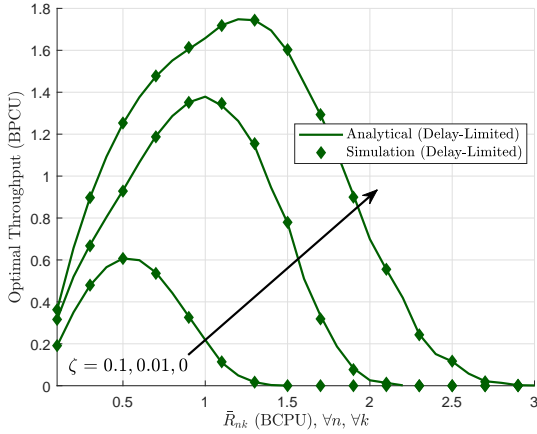


FIGURE 5. Optimal throughput in delay-limited mode versus the target rates and different values of ζ , in which $\bar{\gamma} = 30$ (dB) and $N = 2$.

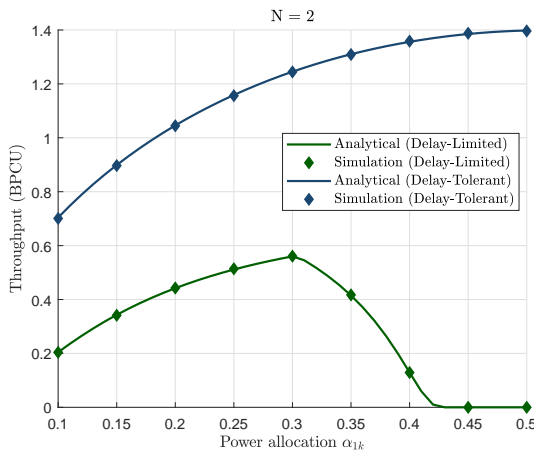


FIGURE 6. Impact of power allocation factor on throughput performance, in which $\bar{R}_{nk} = 0.6$ (BPCU) and $\bar{\gamma} = 30$ (dB).

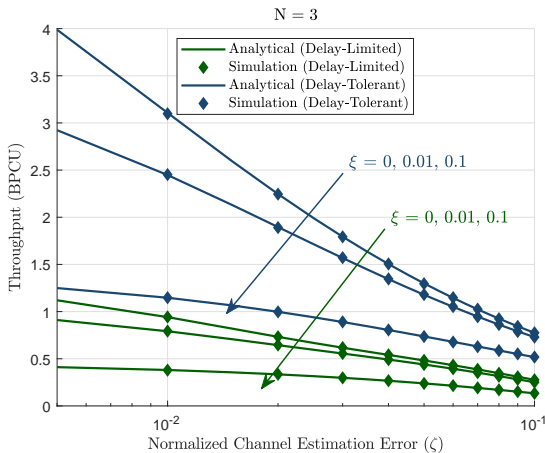


FIGURE 7. Comparison on throughput in two modes, in which $\bar{R}_{nk} = 0.4$ (BPCU) and $\bar{\gamma} = 30$ (dB).

As a comparison in Fig. 7, the NOMA-based multi-pair network in imperfect CSI circumstance depends on the level of channel estimation errors. It is seen that the performance of the multi-pair TWR network with delay-tolerant mode significantly outperforms the counterpart under whole range of channel estimation error.

V. CONCLUSION

In this paper, a NOMA-based multi-pair TWR network has been studied in terms of throughput performance in two transmission modes. The metric of throughput in delay-limited mode and delay-tolerant mode are evaluated to find optimal performance. For each mode, we derived closed-form expressions of outage probability and the corresponding asymptotic performance is also investigated. Extensive simulation results in terms of ergodic rate and outage probability have been provided to validate the superiority of our proposed system under impact of imperfect CSI. Particularly, we have shown that the performance of our proposed system can be improved by reducing the levels of channel estimation error, selecting reasonable numbers of user pairs with appropriate power allocation factors. However, interesting topics such as power allocation optimization, MIMO, practical implementation with imperfect CSI, and novel multiple pair strategies still remain open for future investigations in the NOMA-based TWR network. Integration of these aspects will be studied in the future works.

APPENDIX A PROOF OF LEMMA 1

First, substituting (4) into P_1 , the probability P_1 can be obtained as

$$P_1 = \Pr \left\{ \bigcap_{m=1}^n \beta_{nk} \phi_{nk} \geq \tau_{mk} \right. \\ \left. \times \left(\sum_{m=n+1}^N \beta_{mk} \phi_{mk} + \iota_k + \Delta_k + 1 \right) \right\}. \quad (\text{A.1})$$

Further, the PDF and the CDF of the random variable ϕ_{nk} can be given as

$$f_{\phi_{nk}}(x) = \frac{1}{\hat{\lambda}_{nk}} \exp \left(-\frac{x}{\hat{\lambda}_{nk}} \right), \\ F_{\phi_{nk}}(x) = 1 - \exp \left(-\frac{x}{\hat{\lambda}_{nk}} \right), \quad (\text{A.2})$$

respectively. Due to the fact that ι_k is the sum of independent and non-identically exponentially distributed random variables, i.e., $\beta_{n\bar{k}} |f_{n\bar{k}}^{(1)}|^2$, its PDF can be obtained as [33]

$$f_{\iota_k}(y) = \sum_{n=1}^N \frac{\chi_{n\bar{k}}}{\xi_1 \beta_{n\bar{k}} \lambda_{n\bar{k}}} \exp \left(-\frac{y}{\xi_1 \beta_{n\bar{k}} \lambda_{n\bar{k}}} \right). \quad (\text{A.3})$$

It can be seen that the probability P_1 can be further derived via the following multifold integral

$$P_1 = \int_0^\infty f_{l_k}(y) \int_{L_{Nk}} f_{\phi_{Nk}}(x_{Nk}) \cdots \int_{L_{nk}} f_{\phi_{nk}}(x_{nk}) \cdots \times \int_{L_{1k}} f_{\phi_{1k}}(x_{1k}) dx_{1k} \cdots dx_{nk} \cdots dx_{Nk} dy, \quad (\text{A.4})$$

within each fold, the lower bound of the integration, denoted by L_{mk} with $n \geq m \geq 1$, is given by

$$L_{mk} = \frac{\tau_{mk}}{\beta_{mk}} \left(1 + y + \Delta_k + \sum_{t=m+1}^N \beta_{tk} x_{tk} \right), \quad (\text{A.5})$$

and $L_{mk} = 0$ with $N \geq m \geq n + 1$. For convenience, the integral P_1 can be rewritten as

$$P_1 = \int_0^\infty f_{l_k}(y) g_N(y) dy, \quad (\text{A.6})$$

in which $g_v(y)$ denotes the integral up to the v -th fold of P_1 ($1 \leq v \leq N$) and can be represented by

$$g_v(y) = \int_{L_{vk}}^\infty f_{\phi_{vk}}(x_{vk}) g_{v-1}(y) dx_{vk}, \quad (\text{A.7})$$

in which $g_0(y) = 1$. Subsequently, the first fold of P_1 can be solved with the help of (A.2) and (A.5) as

$$g_1(y) = e^{-\frac{\tau_{1k}}{\beta_{1k}\lambda_{1k}}(\Delta_k+y+1)} \prod_{m=2}^N e^{-\frac{\tau_{1k}}{\beta_{1k}\lambda_{1k}}\beta_{mk}x_{mk}}. \quad (\text{A.8})$$

Solving the second fold, we then obtain

$$g_2(y) = \frac{1}{\beta_{2k}\hat{\lambda}_{2k}} \left(\frac{\tau_{1k}}{\beta_{1k}\hat{\lambda}_{1k}} + \frac{1}{\beta_{2k}\hat{\lambda}_{2k}} \right)^{-1} \times e^{-\left(\frac{\tau_{1k}\tau_{2k}}{\beta_{1k}\hat{\lambda}_{1k}} + \frac{\tau_{2k}}{\beta_{2k}\hat{\lambda}_{2k}} + \frac{\tau_{1k}}{\beta_{1k}\hat{\lambda}_{1k}} \right)(y+\Delta_k+1)} \times \prod_{m=3}^N e^{-\left(\frac{\tau_{1k}\tau_{2k}}{\beta_{1k}\hat{\lambda}_{1k}} + \frac{\tau_{2k}}{\beta_{2k}\hat{\lambda}_{2k}} + \frac{\tau_{1k}}{\beta_{1k}\hat{\lambda}_{1k}} \right)\beta_{mk}x_{mk}}. \quad (\text{A.9})$$

Successively repeating the above process, with the help of the identity Λ_{mk} in (14), the n -th fold of the integral in (A.4) can be expressed as

$$g_n(y) = \prod_{m=1}^n \frac{1}{\beta_{mk}\hat{\lambda}_{mk}\Lambda_{mk}} \times \exp \left(-(y + \Delta_k + 1) \sum_{m=1}^n \tau_{mk}\Lambda_{mk} \right) \times \prod_{t=n+1}^N \exp \left(-\beta_{tk}x_{tk} \sum_{m=1}^n \tau_{mk}\Lambda_{mk} \right). \quad (\text{A.10})$$

For the $(n+1)$ -th till the N -th fold, the lower bound is zero, i.e., $L_{mk} = 0$, thus $g_N(y)$ can be obtained as in (A.11) at the top of this page.

The last integral in (A.4) can then be obtained by substituting (A.11) into (A.6), which then yields

$$P_1 = \prod_{m=1}^n \frac{1}{\beta_{mk}\hat{\lambda}_{mk}\Lambda_{mk}} \exp \left(-(\Delta_k + 1) \sum_{m=1}^n \tau_{mk}\Lambda_{mk} \right) \times \prod_{t=n+1}^N \left(1 + \beta_{tk}\hat{\lambda}_{tk} \sum_{m=1}^n \tau_{mk}\Lambda_{mk} \right)^{-1} \times \int_0^\infty f_{l_k}(y) \exp \left(-y \sum_{m=1}^n \tau_{mk}\Lambda_{mk} \right) dy. \quad (\text{A.12})$$

Substituting (A.3) into the above equation and then solving the resulted integral, we then obtain

$$P_1 = \prod_{m=1}^n \frac{1}{\beta_{mk}\hat{\lambda}_{mk}\Lambda_{mk}} \exp \left(-(\Delta_k + 1) \sum_{m=1}^n \tau_{mk}\Lambda_{mk} \right) \times \prod_{t=n+1}^N \left(1 + \beta_{tk}\hat{\lambda}_{tk} \sum_{m=1}^n \tau_{mk}\Lambda_{mk} \right)^{-1} \times \sum_{n=1}^N \chi_{t\bar{k}} \left(1 + \xi_1 \beta_{tk}\hat{\lambda}_{t\bar{k}} \sum_{m=1}^n \tau_{mk}\Lambda_{mk} \right)^{-1}. \quad (\text{A.13})$$

At this point, we then derive the probability P_2 , which is, from (14), is equivalent to

$$P_2 = \prod_{m=1}^n \Pr \left\{ \bigcap_{t=n}^N \frac{\alpha_{t\bar{k}}\phi_{mk}}{\hat{\alpha}_{t\bar{k}}\phi_{mk} + l_{mk} + \Delta_{mk} + 1} \geq \tau_{t\bar{k}} \right\} = \prod_{m=1}^n \Pr \left\{ \bigcap_{t=n}^N \phi_{mk} \geq \frac{\tau_{t\bar{k}}}{\alpha_{t\bar{k}} - \tau_{t\bar{k}}\hat{\alpha}_{t\bar{k}}} (l_{mk} + \Delta_{mk} + 1) \right\} = \prod_{m=1}^n \Pr \{ \phi_{mk} \geq \theta_{n\bar{k}}(l_{mk} + \Delta_{mk} + 1) \}, \quad (\text{A.14})$$

for $\alpha_{t\bar{k}}/\hat{\alpha}_{m\bar{k}} > \tau_{t\bar{k}}, \forall t \in [n, N]$. In addition, the probability P_2 can be further expressed as

$$P_2 = \prod_{m=1}^n \int_0^\infty e^{-\frac{\theta_{n\bar{k}}}{\lambda_{mk}}(y+\Delta_{mk}+1)} f_{l_{mk}}(y) dy, \quad (\text{A.15})$$

where $f_{l_{mk}}(y)$ specifies the PDF of the aggregated interference power at the user D_{mk} from the users in the group $G_{\bar{k}}$, which can be given by

$$f_{l_{mk}}(y) = \frac{1}{\xi_2\lambda_{n\bar{k}}} \exp \left(-\frac{y}{\xi_2\lambda_{n\bar{k}}} \right), \quad y > 0. \quad (\text{A.16})$$

Substituting $f_{l_{mk}}(y)$ in the above equation into (A.14) and solving the integral, we obtain

$$P_2 = \prod_{m=1}^n \left(1 + \frac{\xi_2\lambda_{mk}}{\hat{\lambda}_{mk}}\theta_{n\bar{k}} \right)^{-1} e^{-\frac{\theta_{n\bar{k}}(\Delta_{mk}+1)}{\lambda_{mk}}}. \quad (\text{A.17})$$

Finally, by substituting (A.13) and (A.17) into $P_{nk}^{ip,out}$ in (9), we then obtain Lemma 1. This is the end of the proof.

$$\begin{aligned}
 g_N(y) &= \prod_{m=1}^n \frac{1}{\beta_{mk} \hat{\lambda}_{mk} \Lambda_{mk}} e^{-(\Delta_k+y+1) \sum_{m=1}^n \tau_{mk} \Lambda_{mk}} \prod_{t=n+1}^N \int_0^\infty f_{\phi_{tk}}(x_{tk}) e^{-\beta_{tk} x_{tk} \sum_{m=1}^n \tau_{mk} \Lambda_{mk}} dx_{tk}, \\
 &= \prod_{m=1}^n \frac{1}{\beta_{mk} \hat{\lambda}_{mk} \Lambda_{mk}} e^{-(\Delta_k+y+1) \sum_{m=1}^n \tau_{mk} \Lambda_{mk}} \prod_{t=n+1}^N \left(1 + \beta_{tk} \hat{\lambda}_{tk} \sum_{m=1}^n \tau_{mk} \Lambda_{mk} \right)^{-1}. \quad (\text{A.11})
 \end{aligned}$$

APPENDIX B PROOF OF LEMMA 2

The CDF of X_{nk} is given by

$$\begin{aligned}
 F_{X_{nk}}(z) &= \Pr\{X_{nk} < z\} \\
 &= 1 - \Pr\{\gamma_{R \rightarrow x_{nk}} \geq z\} \prod_{m=1}^n \Pr\{\gamma_{m\bar{k} \rightarrow nk} \geq z\}. \quad (\text{B.1})
 \end{aligned}$$

Denoting the first and second probabilities in (B.1) as $P_1(z)$ and $P_2(z)$, respectively. Substituting (4) into $P_1(z)$ and after some probabilistic approaches, $P_1(z)$ can then be derived as

$$\begin{aligned}
 P_1(z) &= \exp\left(-\frac{z}{\beta_{nk} \hat{\lambda}_{nk}} (\Delta_k + 1)\right) \quad (\text{B.2}) \\
 &\times \underbrace{\int_0^\infty f_{t_k}(y) \exp\left(-\frac{z}{\beta_{nk} \hat{\lambda}_{nk}} y\right) dy}_{I_1(z)} \\
 &\times \prod_{m=n+1}^N \underbrace{\int_0^\infty \frac{f_{\phi_{mk}}\left(\frac{x}{\beta_{mk}}\right)}{\beta_{mk}} \exp\left(-\frac{z}{\beta_{nk} \hat{\lambda}_{nk}} x\right) dx}_{I_2(z)},
 \end{aligned}$$

Using (A.3), the first integral part can be evaluated as

$$I_1(z) = \sum_{t=1}^N \chi_{t\bar{k}} \left(1 + \frac{\beta_{t\bar{k}} \lambda_{t\bar{k}}}{\beta_{nk} \hat{\lambda}_{nk}} \xi_1 z \right)^{-1}, \quad z > 0, \quad (\text{B.3})$$

Substituting (A.2) into I_2 , the second integral is derived as

$$I_2(z) = \left(1 + \frac{\beta_{mk} \hat{\lambda}_{mk}}{\beta_{nk} \hat{\lambda}_{nk}} z \right)^{-1}, \quad z > 0, \quad (\text{B.4})$$

From (B.3) and (B.4) the first probability in (B.1) is then given by

$$P_1(z) = e^{-(\Delta_k+1) \frac{z}{\beta_{nk} \hat{\lambda}_{nk}}} I_1(z) \prod_{m=n+1}^N I_2(z). \quad (\text{B.5})$$

For the second probability at $z < \alpha_{nk}/\hat{\alpha}_{nk}$, i.e., $P_2(z)$, with (8) and after some steps, we can obtain

$$P_2(z) = \Pr\{\phi_{m\bar{k}} \geq \varepsilon_{nk}(z)(l_{m\bar{k}} + \Delta_{m\bar{k}} + 1)\}, \quad (\text{B.6})$$

Substituting the complementary CDF $\phi_{m\bar{k}}$, the PDF of $l_{m\bar{k}}$ and with $\hat{\lambda}_{m\bar{k}}/\lambda_{m\bar{k}} = 1 - \zeta_{m\bar{k}}$, (C.2) can be further derived as

$$P_2(z) = e^{-(\Delta_k+1) \frac{z}{\beta_{nk} \hat{\lambda}_{nk}}} \left(1 + \frac{\xi_2}{1 - \zeta_{m\bar{k}}} \varepsilon_{nk}(z) \right)^{-1} \quad (\text{B.7})$$

Substituting (B.5) and (B.7) into (B.1), we then obtain the result in Lemma 2. This is the end of the proof.

APPENDIX C PROOF OF PROPOSITION 3

Substituting (18) into (19) yields

$$\begin{aligned}
 R_{1k}^{erg} &= \frac{1}{2\ln 2} \sum_{t=1}^N \chi_{t\bar{k}} \int_0^\infty \frac{e^{-\mu_{1k}\gamma}}{1+\gamma} \left(1 + \frac{\beta_{t\bar{k}} \lambda_{t\bar{k}}}{\beta_{1k} \hat{\lambda}_{1k}} \xi_1 z \right)^{-1} \\
 &\times \prod_{m=2}^N \left(1 + \frac{\beta_{mk} \hat{\lambda}_{mk}}{\beta_{1k} \hat{\lambda}_{1k}} z \right)^{-1} \left(1 + \frac{\lambda_{1\bar{k}}}{\alpha_{1k} \hat{\lambda}_{1\bar{k}}} \xi_2 \gamma \right)^{-1} d\gamma. \quad (\text{C.1})
 \end{aligned}$$

It is noted that the product term can be rewritten into the following finite sum via decomposition such that

$$\prod_{m=2}^N \left(1 + \frac{\beta_{mk} \hat{\lambda}_{mk}}{\beta_{1k} \hat{\lambda}_{1k}} z \right)^{-1} = \sum_{m=2}^N \psi_{mk} \left(1 + \frac{\beta_{mk} \hat{\lambda}_{mk}}{\beta_{1k} \hat{\lambda}_{1k}} z \right)^{-1}.$$

Substituting the above equation into (C.1) yields

$$\begin{aligned}
 R_{1k}^{erg} &= \frac{1}{2\ln 2} \sum_{t=1}^N \chi_{t\bar{k}} \sum_{m=2}^N \psi_{mk} \quad (\text{C.2}) \\
 &\times \int_0^\infty \frac{e^{-\mu_{1k}\gamma}}{(1+\varpi_1\gamma)(1+\varpi_2\gamma)(1+\varpi_3\gamma)(1+\varpi_4\gamma)} d\gamma.
 \end{aligned}$$

Using partial fraction to decompose the product terms in the integral, we then obtain

$$\begin{aligned}
 R_{1k}^{erg} &= \frac{1}{2\ln 2} \sum_{t=1}^N \chi_{t\bar{k}} \sum_{m=2}^N \psi_{mk} \left(\int_0^\infty \frac{\vartheta_1}{1+\varpi_1\gamma} e^{-\mu_{1k}\gamma} d\gamma \right. \\
 &+ \int_0^\infty \frac{\vartheta_2}{1+\varpi_2\gamma} e^{-\mu_{1k}\gamma} d\gamma + \int_0^\infty \frac{\vartheta_3}{1+\varpi_3\gamma} e^{-\mu_{1k}\gamma} d\gamma \\
 &\left. + \int_0^\infty \frac{\vartheta_4}{1+\varpi_4\gamma} e^{-\mu_{1k}\gamma} d\gamma \right). \quad (\text{C.3})
 \end{aligned}$$

Applying the identity [34, Eq. (3.352.4)], into the above integrals, one then can obtain (20). This is the end of the proof.

REFERENCES

- [1] R. H. Tehrani, S. Vahid, D. Triantafylloupolou, H. Lee, and K. Moessner, "Licensed spectrum sharing schemes for mobile operators: A survey and outlook," *IEEE Commun. Surveys Tuts.*, vol. 18, no. 4, pp. 2591–2623, 4th Quart., 2016.
- [2] Dinh-Thuan Do, A. Le and B. M. Lee, "NOMA in Cooperative Underlay Cognitive Radio Networks Under Imperfect SIC," *IEEE Access*, vol. 8, pp. 86180–86195, 2020.
- [3] S. M. R. Islam, N. Avazov, O. A. Dobre and K. Kwak, "Power-Domain Non-Orthogonal Multiple Access (NOMA) in 5G Systems: Potentials and Challenges," *IEEE Communications Surveys & Tutorials*, vol. 19, no. 2, pp. 721–742, Secondquarter 2017.
- [4] M. Zeng, A. Yadav, O. A. Dobre, G. I. Tsiropoulos and H. V. Poor, "On the Sum Rate of MIMO-NOMA and MIMO-OMA Systems," *IEEE Wireless Communications Letters*, vol. 6, no. 4, pp. 534–537, Aug. 2017.

- [5] M. Zeng, A. Yadav, O. A. Dobre, G. I. Tsiropoulos, and H. V. Poor, "Capacity comparison between MIMO-NOMA and MIMO-OMA with multiple users in a cluster," *IEEE J. Sel. Areas Commun.*, vol. 35, no. 10, pp. 2413–2424, Oct. 2017.
- [6] X. Tang, K. An, K. Guo, Y. Huang, and S. Wang, "Outage analysis of non-orthogonal multiple access-based integrated satellite-terrestrial relay networks with hardware impairments," *IEEE ACCESS*, vol. 7, pp. 141258–141267, Sep. 2019.
- [7] M. Moltafet, N. Mokari, M. Reza Javan and P. Azmi "Comparison Study between PD-NOMA and SCMA," *IEEE Transactions on Vehicular Technology*, vol. 67, no.2, 2018.
- [8] M. Moltafet, N. Mokari, M. R. Javan, H. Saeedi, and H. Pishro-Nik, "A New Multiple Access Technique for 5G: Power Domain Sparse Code Multiple Access (PSMA)," *IEEE Access*, vol. 6, 2018.
- [9] M. Moltafet, S. Parsaeefard, M. Reza Javan, N. Mokari "Robust Radio Resource Allocation in MISO-SCMA Assisted C-RAN in 5G Networks," *IEEE Trans. on Vehicular Technology*, vol. 68, no. 6, 2019.
- [10] A. S. Ibrahim, A. K. Sadek, W. Su, et al. Cooperative communications with relay-selection: when to cooperate and whom to cooperate with?. *IEEE Trans. Wireless Commun.* 2008, 7, 2814–2827.
- [11] X. Wu, M. Lin, H. Kong, Q. Huang, J. Y. Wang, P. K. Upadhyay, "Outage Performance for Multiuser Threshold-based DF Satellite Relaying," *IEEE Access*, vol. 7, no. 1, pp 103142–103152, Dec. 2019.
- [12] T.-L. Nguyen and D.-T. Do, "Power Allocation Schemes for Wireless Powered NOMA Systems with Imperfect CSI: System model and performance analysis," *International Journal of Communication Systems*, vol. 31, no. 15, e3789, 2018.
- [13] D.-T. Do, A.-T. Le, C.-B. Le and B.M. Lee. "On Exact Outage and Throughput Performance of Cognitive Radio based Non-Orthogonal Multiple Access Networks With and Without D2D Link." *Sensors*, vol. 19, no. 15: 3314.
- [14] X. Yue, Y. Liu, S. Kang, and A. Nallanathan, "Performance Analysis of NOMA With Fixed Gain Relaying Over Nakagami- m Fading Channels," *IEEE Access*, vol. 5, pp. 5445–5454, 2017.
- [15] D.-T. Do and A.-T. Le. NOMA based cognitive relaying: Transceiver hardware impairments, relay selection policies and outage performance comparison. *Computer Communications*, 146, pp.144–154, 2019.
- [16] Dinh-Thuan Do and M.-S. Van Nguyen. Device-to-device transmission modes in NOMA network with and without Wireless Power Transfer. *Computer Communications*, vol. 139, pp. 67–77, 2019.
- [17] D.-T. Do, A.-T. Le and B.-M. Lee. "On Performance Analysis of Underlay Cognitive Radio-Aware Hybrid OMA/NOMA Networks with Imperfect CSI." *Electronics* 8, no. 7: 819, 2019.
- [18] Dinh-Thuan Do, "Power Switching Protocol for Two-way Relaying Network under Hardware Impairments," *Radioengineering*, vol. 24 , no. 3, pp. 765-771, 2015.
- [19] K. Guo, K. An, B. Zhang, D. Guo, "Performance analysis of two-way satellite multi-terrestrial relay networks with hardware impairments," *Sensors*, vol. 18, vol 5, pp. 1-18, May 2018.
- [20] J. Bae and Y. Han, "Joint Power and Time Allocation for Two-Way Cooperative NOMA," in *IEEE Trans. Veh. Technol.*, vol. 68, no. 12, pp. 12443–12447, Dec. 2019.
- [21] F. Wei, T. Zhou, T. Xu and H. Hu, "Modeling and Analysis of Two-Way Relay Networks: A Joint Mechanism Using NOMA and Network Coding," *IEEE Access*, vol. 7, pp. 152679–152689, 2019.
- [22] B. Zheng, X. Wang, M. Wen and F. Chen, "NOMA-Based Multi-Pair Two-Way Relay Networks With Rate Splitting and Group Decoding," in *IEEE J. Sel. Areas Commun.*, vol. 35, no. 10, pp. 2328–2341, Oct. 2017.
- [23] B. Zheng et al., "Secure NOMA Based Two-Way Relay Networks Using Artificial Noise and Full Duplex," in *IEEE J. Sel. Areas Commun.*, vol. 36, no. 7, pp. 1426–1440, July 2018.
- [24] X. Li, J. Li and L. Li, "Performance Analysis of Impaired SWIPT NOMA Relaying Networks Over Imperfect Weibull Channels," *IEEE Systems Journal*. doi: 10.1109/JSYST.2019.2919654
- [25] Z. Yang, Z. Ding, P. Fan and G. K. Karagiannidis, "On the Performance of Non-orthogonal Multiple Access Systems With Partial Channel Information," in *IEEE Trans. Commun.*, vol. 64, no. 2, pp. 654–667, Feb. 2016..
- [26] J. Men, J. Ge and C. Zhang, "Performance Analysis for Downlink Relaying Aided Non-Orthogonal Multiple Access Networks With Imperfect CSI Over Nakagami- m Fading," in *IEEE Access*, vol. 5, pp. 998–1004, 2017.
- [27] B. Xia, Y. Liu, C. Yang, Z. Chen, W. Xie and Y. Zhao, "Opportunistic Channel Sharing in Stochastic Networks With Dynamic Traffic," in *IEEE Trans. Veh. Technol.*, vol. 66, no. 10, pp. 9587–9591, Oct. 2017..
- [28] S. Arzykulov, T. A. Tsiftsis, G. Nauryzbayev and M. Abdallah, "Outage Performance of Cooperative Underlay CR-NOMA With Imperfect CSI," in *IEEE Commun. Lett.*, vol. 23, no. 1, pp. 176–179, Jan. 2019..
- [29] S. Xie, B. Zhang, D. Guo and W. Ma, "Outage performance of NOMA-based integrated satellite-terrestrial networks with imperfect CSI," in *Electronics Lett.*, vol. 55, no. 14, pp. 793–795, 11 7 2019.
- [30] J. Cui, Z. Ding and P. Fan, "Outage Probability Constrained MIMO-NOMA Designs Under Imperfect CSI," in *IEEE Trans. Wireless Commun.*, vol. 17, no. 12, pp. 8239–8255, Dec. 2018.
- [31] F. Fang, H. Zhang, J. Cheng, S. Roy and V. C. M. Leung, "Joint User Scheduling and Power Allocation Optimization for Energy-Efficient NOMA Systems With Imperfect CSI," in *IEEE J. Sel. Areas Commun.*, vol. 35, no. 12, pp. 2874–2885, Dec. 2017.
- [32] X. Yue, Y. Liu, S. Kang, A. Nallanathan and Y. Chen, "Modeling and Analysis of Two-Way Relay Non-Orthogonal Multiple Access Systems," *IEEE Trans. on Commun.*, vol. 66, no. 9, pp. 3784–3796, Sep. 2018.
- [33] A. Bletsas, H. Shin and M. Z. Win, "Cooperative Communications with Outage-Optimal Opportunistic Relaying," in *IEEE Trans. Wireless Commun.*, vol. 6, no. 9, pp. 3450–3460, September 2007.
- [34] I. S. Gradshteyn and I. M. Ryzhik, *Table of Integrals, Series and Products*, 6th ed. New York: Academic Press, 2000.



DINH-THUAN DO received the B.S.degree, M.Eng. degree, and Ph.D. degree from Viet Nam National University (VNU-HCM) in 2003, 2007, and 2013 respectively, all in Communications Engineering. He was a visiting Ph.D. student with Communications Engineering Institute, National Tsing Hua University, Taiwan from 2009 to 2010. Prior to joining Ton Duc Thang University, he was senior engineer at the VinaPhone Mobile Network from 2003 to 2009. Dr. Thuan was recipient of

Golden Globe Award from Vietnam Ministry of Science and Technology in 2015 (Top 10 excellent young scientists nationwide). His research interest includes signal processing in wireless communications network, cooperative communications, Non-Orthogonal Multiple Access, full-duplex transmission and energy harvesting.

He published over 65 SCI/SCIE journal papers, two book chapters and one sole author book. He served as a lead Guest Editor in the Special Issue "Recent Advances for 5G: Emerging Scheme of NOMA in Cognitive Radio and Satellite Communications" in *ELECTRONICS* (2019) and as a Guest Editor in the Special Issue on "Massive sensors data fusion for healthcare informatics" in (Springer) *ANNALS OF TELECOMMUNICATIONS* (2020). Dr. Thuan is currently serving as an Associate Editor in 6 journals, in which main journals are *EURASIP JOURNAL ON WIRELESS COMMUNICATIONS AND NETWORKING*, *COMPUTER COMMUNICATIONS (ELSERVIER)* and *KSII TRANSACTIONS ON INTERNET AND INFORMATION SYSTEMS*.



THANH-LUAN NGUYEN received his First class B.S. from Ho Chi Minh City University of Technology and Education, Viet Nam, 2016. He currently is a Research Assistant in Industrial University of Ho Chi Minh City (IUH), Faculty of Electronics Technology. His research interests include NOMA, Energy Harvesting, Generalized Channels and other emerging technologies.



KHALED M. RABIE received the B.S. degree (Hons.) from Tripoli University, Libya, in 2008, the M.Sc. degree from the University of Manchester, Manchester, U.K., in 2010, and the Ph.D. degree in electrical and electronic engineering from the University of Manchester, in 2015. He joined the Manchester Metropolitan University (MMU), U.K., where he is currently an Assistant Professor with the Department of Engineering. He has published more than 90 articles in prestigious journals

and international conferences, and serves regularly on the Technical Program Committee of several major IEEE conferences such as GLOBECOM, ICC, VTC, and so on. His primary research focuses on various aspects of the next-generation wireless communication systems. Dr. Rabie is also a Fellow of the U.K. Higher Education Academy (FHEA). He has received numerous awards over the past few years in recognition of his research contributions including the Best Student Paper Award at the IEEE ISPLC, TX, USA, 2015, the MMU Outstanding Knowledge Exchange Project Award of 2016, and the IEEE Access Editor of the month award for August 2019. He currently serves as an Associate Editor of IEEE ACCESS, an Area Editor of Physical Communication (Elsevier), and an Executive Editor of Transactions on Emerging Telecommunications Technologies (Wiley).



BYUNG MOO LEE received the Ph.D. degree in Electrical and Computer Engineering from the University of California, Irvine, CA, USA, in 2006. He is currently an Associate Professor in the School of Intelligent Mechatronics Engineering at Sejong University, Seoul, South Korea. Prior to joining Sejong University, he had ten years of industry experience including research positions at the Samsung Electronics Seoul R&D Center, Samsung Advanced Institute of Technology, and Korea Telecom R&D Center. During his industry experience, he participated in IEEE 802.16/11, Wi-Fi Alliance, and 3GPP LTE standardizations, and also participated in Mobile VCE and Green Touch Research Consortiums where he made numerous contributions and filed a number of related patents. His research interests are in the areas of wireless communications, signal processing, and machine learning applications.

Dr. Lee served as a Vice Chairman of the Wi-Fi Alliance Display MTG in 2015-2016.

...



XINGWANG LI received the B.Sc. degree from Henan Polytechnic University, in 2007, the M.Sc. degree from the University of Electronic Science and Technology of China, in 2010, and the Ph.D. degree from the Beijing University of Posts and Telecommunications, in 2015. From 2010 to 2012, he was with Comba Telecom Ltd., Guangzhou, China, as an Engineer. From 2017 to 2018, he was a Visiting Scholar with Queen's University Belfast, Belfast, U.K. He is also a Visiting Scholar

with the State Key Laboratory of Networking and Switching Technology, Beijing University of Posts and Telecommunications, from 2016 to 2018. He is currently an Associate Professor with the School of Physics and Electronic Information Engineering, Henan Polytechnic University, Jiaozuo China. His research interests include MIMO communication, cooperative communication, hardware constrained communication, non-orthogonal multiple access, physical layer security, unmanned aerial vehicles, and the Internet of Things. He is also the Co-Chair of IEEE/IET CSNDSP 2020 of the Green Communications and Networks track. He is currently an Editor on the Editorial Board of IEEE ACCESS, Computer Communications, and KSII Transactions on Internet and Information Systems. He is also the Lead Guest Editor for the special issue on Recent Advances in Physical Layer Technologies for the 5G-Enabled Internet of Things of the Wireless Communications and Mobile Computing. He has served as many TPC members, such as IEEE/CIC, GLOBECOM, WCNC, and so on.